

KAMARPOSHTI, M.A., COLAK, I., IWENDI, C., BAND, S.S. and IBEKE, E. 2022. Optimal coordination of PSS and SSSC controllers in power system using ant colony optimization algorithm. *Journal of circuits, systems and computers* [online], 31(4), article 2250060. Available from: <https://doi.org/10.1142/S0218126622500608>

Optimal coordination of PSS and SSSC controllers in power system using ant colony optimization algorithm.

KAMARPOSHTI, M.A., COLAK, I., IWENDI, C., BAND, S.S. and IBEKE, E.

2022

Electronic version of an article published as *Journal of Circuits, Systems, and Computers*, 31(4), article 2250060, 2022, <https://doi.org/10.1142/S0218126622500608>. © World Scientific Publishing Company
<https://www.worldscientific.com/worldscinet/jcsc>.

Optimal Coordination of PSS and SSSC Controllers in Power System Using Ant Colony Optimization Algorithm

Mehrdad Ahmadi Kamarposhti*

*Department of Electrical Engineering, Jouybar Branch, Islamic Azad University, Jouybar, Iran
Corresponding Author Email: mehrdad.ahmadi.k@gmail.com*

Ilhami Colak

Department of Electrical and Electronics, Faculty of Engineering and Architectures, Nisantasi University, Istanbul, Turkey

Celestine Iwendi

*School of Creative Technologies, University of Bolton, United Kingdom
celestine.iwendi@ieee.org*

Shahab S. Band†

*Future Technology Research Center, College of Future, National Yunlin University of Science and Technology,
123 University Road
Yunlin 64002, Taiwan
shamshirbands@yuntech.edu.tw*

Ebuka Ibeke‡

*School of Creative and Cultural Business, Robert Gordon University, United Kingdom
e.ibeke@rgu.ac.uk*

Received (Day Month Year)

Revised (Day Month Year)

Accepted (Day Month Year)

Volatility leads to disruption in synchronism between generators of a continuous system. The frequency of the volatility is usually between a few tenths of Hz to several Hz. This volatility is sometimes divided into two types, local and interregional. Local volatility is the low-frequency volatility of a power plant unit or units of a power plant relative to the grid whereas interregional volatility is the volatility of the units of one area relative to the units of another area. The worst kind of low-frequency volatility occurs when the power system in a region has a short three-phase connection to the earth, creating a complete instability of the grid and operating protective systems. One of the ways to improve the dynamic stability and steady-state of the power system is to use power system stabilizers and FACTS devices in the system. In this paper, the stabilization of the power system stabilizers PSS and SSSC is done using the ant colony algorithm. Studies on a four-machine system with the three-phase error were performed in two scenarios and finally compared with the PSO method. The simulation results show that the proposed method produced more accurate performance.

* Corresponding author

† Corresponding author

‡ Corresponding author

Keywords: PSS, SSSC, Cost Reduction, FACTS devices, low-frequency volatility, Ant Colony Optimization Algorithm.

1. Introduction

The stability of power systems has become an important area of study, this is mostly due to the integration of power systems. As a result, more advanced control equipment and stronger protection schemes have been added to the power system to increase stability. However, new stability issues have been posed and analysis becomes more difficult. Early in the development of power systems, instability issues were mainly due to the lack of synchronizing torque. Therefore, the purpose of stability enhancement was to limit the amplitude of the first rotor angle volatility in transient stability and to increase the steady-state power transmission range. Significant improvement in the operation of the power system led to issues such as the stability of the small disturbance of the local volatility model, and low-frequency interregional volatility modes were revealed. Many factors can cause volatility in the grid, such factors include a short connection in the grid, sudden change of load or interruption of load or loss of transmission lines. These volatilities can occur in the normal operating state of the system. The ability of the power system to maintain stability depends largely on the stabilizing equipment available on the power system. One of these methods is the use of an auxiliary control loop on machine excitation, known as the power system stabilizer (PSS). The damping rate added through this is limited due to the time constant of the stimulation and saturation problems. In addition, in this method, a feedback state is taken from feedback and added to the stimulation and the effect of other state variables is not considered. To introduce the effect of other state variables, it is necessary to insert a signal composed of the linear combination of state variables into the stimulation system; to obtain the coefficients of the state variables, optimal control is used.

Another way to improve the dynamic stability and steady-state of the power system is to use the flexible alternating current transmission system (FACTS) devices in the system. FACTS devices, as active and reactive power compensators in power systems, can improve reliability and efficiency due to their rapid response to disturbance and their flexible performance under normal system conditions [1]. FACTS technology provides new opportunities for controlling power and increasing the usable capacity of existing lines as well as new lines. The use of FACTS controller devices enables the control of power distribution within the lines under normal and unforeseen conditions. These opportunities are made possible by the ability of FACTS controllers to control the parameters that direct the performance of the transmission system in relation to each other; parameters such as series impedance, parallel impedance, current, voltage, voltage angle, and damping of volatility at different frequencies below the system nominal frequency [1]. Series static synchronous compensator (SSSC) is one of the best suggestions for damping power system volatility. A static synchronous generator that operates as a series compensator without an external power supply, and its output voltage is 90 degrees phase difference with the line current and can be controlled independently from the line current to increase or decrease

the total reactive voltage drop is used along the line to control the transmitted electrical power. SSSC may include a transient amount of energy storage or energy absorption devices to temporarily increase the power system's performance by compensating extra real power and temporarily increasing or decreasing the total actual voltage drop (resistive voltage drop) along the line.

In recent years, numerous studies have been carried out on the different types of power system stability. In all these investigations, the researchers tried to improve the stimulation system and FACTS stimulation through stabilizer control in a stable way. A major share of this research is concerned with the design of PSS stabilizers or the control of FACTS devices in the power system or the context of the coordination between the power system stabilizer and the FACTS devices. Many methods and algorithms such as genetics, turbulence, bee colonies, particle consensus, etc. have been applied to the PSS stabilizer design, each of which has strengths and weaknesses.

A genetic algorithm is used in [2] to find optimal parameters of power system stabilizers, i.e., K_{stab} , T_1 , T_2 , T_3 and T_4 coefficients. In this reference, the coefficients of participation are first used to determine the location of stabilizers and then using the genetic algorithm, the number of stabilizers is reduced and finally, the genetic algorithm presents the optimal model of the stabilizer. In [3], the particle swarm optimization (PSO) algorithm is used to optimally design the stabilizers as well as their placement in the power system to reduce interregional volatility. In [4], the particle aggregation algorithm of the power system stabilizer (PSS) parameters is used at the grid point. It is then carried out by the fuzzy system of the stabilizer in the power system. Stabilizers designed in the two-region, four-machine standard system, have been used and it has been claimed that the volatility of interregional and within regional have been reduced. Another group of power engineers has been involved in the coordination of power system stabilizers as well as controlling FACTS devices. In [5], PSS and thyristor-controlled series compensator (TCSC), the PSO algorithm is used to coordinate them. Also, in [6], static VAR compensator (SVC) and TCSC compensator optimized by PSO algorithm in power system is used.

Another algorithm used in recent articles is the bacterial foraging optimization algorithm (BFOA). This has been used more to find optimal points because of its high accuracy. In [7], synchronization between the stabilizers of the PSSs power system and SVC is performed by the bacterial foraging optimization algorithm. Finally, with the coordination of the controllers in the power system, interregional volatility obtained acceptable damping. Also, in [8], this algorithm was used for the optimal design of the power system stabilizer. In [9], a modified version of the bacterial foraging optimization algorithm was used to optimally design the PSS stabilizer and TCSC line compensator. The authors claimed that the modified version of the BFOA algorithm has high convergence accuracy and speed. In [10–12], the combination of PSO and BFOA was used to precisely design a power system stabilizer. In these papers, it is claimed that the hybrid algorithm has higher accuracy than the PSO algorithm and is not trapped in local optimal points. In [13–18], various applications of Blockchain in the computing system are discussed.

In [19], the duck pack algorithm is used to determine the stabilizing parameters of the post-phase and pre-phase power systems. In the paper, the objective function is defined based on the displacement of the eigenvalues, and the algorithm attempts to provide the stability of the power system over a wide range of generator operating conditions by the replacement of the eigenvalues. The results obtained by the duck pack algorithm are compared with the results of the particle aggregation algorithm. In [20], the duck pack algorithm is used to design stabilizers in a three-machine power system and its results are compared with a system optimized by the genetic algorithm. The results show that the duck pack algorithm performs better than the genetic algorithm. In [21-25], the benefits and applications of the Internet of Things in improving the system are discussed. In [26], a hybrid algorithm based on the bee colony algorithm is used to optimally design power system stabilizers. Also in [27], the author has used the Multi-objective Modified Honey Bee Mating Optimization algorithm to solve the problem of dynamic stability of the power system. In [27], the integral square time square error (ISTSE) criterion, as well as the eigenvalues, is considered objective functions. In this algorithm, like the multi-objective particle swarm optimization (MOPSO) algorithm, the dominant responses are obtained in the Pareto front. The curve of the angular velocity variations obtained from the simulation before the error has the volatility that can be attributed as an error in the results of the paper. In [28], the search optimum algorithm (SOA) has been used to optimally design PSS stabilizers and coordinate them with static synchronous series compensator (SSSC). In [28] a new objective function is proposed. The proposed objective function is a function with the weighted coefficients from the two ISTSE objective functions and a combined function of overshoot, undershoot and settling time. In the paper, it is claimed that the stabilizer designed by minimizing the proposed objective function is more accurate than other methods. In [29], power system stabilizers have been coordinated to reduce interregional mode volatility by a hybrid method of optimization and sensitivity analysis of eigenvalues. This combination allows for a different PSS stabilizer design where the target function reaches its minimum value. To prove the robustness of the proposed method, the stabilizers designed in the 69 generator system were used. A detection system for rumours was discussed in [30]. In [31], a hybrid algorithm of particle swarm and gravitational search algorithm (GSA) were used to design the stabilizer of the PSS power system as well as the coordination between the power system stabilizer and the SSSC compensator. The hybrid algorithm has higher accuracy than both PSO and GSA. The simulation results on the multi-machine system indicate the robust performance of the control system designed in damping low-frequency volatility. The optimal tuning of PSSs and FACTS devices for power system stability enhancement has been also addressed in [32-35]. In [33], the optimal combination of TCSC, SVC and PSSs has been investigated for the suppression of LFOs where the parameters of controllers are optimized based on eigenvalue analysis. Dey et al. [34] have studied the contribution of SVC and TCSC on the small-signal stability of a power network incorporating wind farm, where eigenvalue analysis and time-domain simulation (TDS) have been conducted for various disturbance scenarios. A comprehensive study of the impacts of PSS and unified power flow controller (UPFC) for

the enhancement of power system stability has been presented in [35]. In other studies, the optimal allocation of FACTS devices along with the optimal coordination between these devices and PSSs regulators has been investigated [36, 37]. In [38] is proposed a new optimized interval type-II fuzzy set (T2FS) based on PSS to increase the stability margin of the well-known four-machine power system of a wind farm. In [38] the MOPSO algorithm is employed to design and optimize the membership functions of the proposed stabilizers when integral square error until settling (ISEUS) and figure of demerit (FD) criteria are considered as objective functions.

In all these proposed studies, the issue that has great importance is the adjustment of the PSS and SSSC parameters. In this paper, the ant colony optimization algorithm will be used to coordinate the power system stabilizers and the SSSC. ACO algorithm with high convergence and acceptable accuracy can be a good way to solve the problem of stabilizer coordination and SSSC. In the second part of this paper, the modeling of the problem is discussed. The objective function of the problem is stated in this section. Section 3 briefly describes the ACO optimization algorithm. The simulation results are presented in the form of two scenarios in Section 4. Finally, this paper concludes by presenting the results in Section 5.

2. Problem Modeling

The precise coordination of stabilizers in the power system is an optimization problem that requires the use of an appropriate objective function. Both the ISTSE criteria and the FD have been used as objective functions for designing stabilizers and for coordinating. The ISTSE criterion is defined in Equation 1. The smaller the value of this criterion, the better the condition of the dynamic stability of the system; the volatility also damps with a lower range and shorter time.

$$ISTSE = \int_0^{t_{sim}} ((t \Delta w_{12})^2 + (t \Delta w_{13})^2 + (t \Delta w_{14})^2 + (t \Delta w_{34})^2) dt \quad (1)$$

In the above equation, Δw_{12} , Δw_{13} , Δw_{14} are the rotational angular velocity changes of the first generators to the second, third and fourth generators, respectively. Also, Δw_{34} is the angular velocity difference of the third and fourth generators located in the second region. In Equation 1, the operator t represents the time and t_{sim} of the simulation time equal to 10 seconds. The simulation time should continue until the volatility dampens. The FD criterion is defined as Equation 2.

$$FD = \frac{\sum_{i=1}^{N_G} ((500 \times OS_i)^2 + (8000 \times US_i)^2 + 0.01 \times T_{si}^2)}{N_G} \quad (2)$$

In Equation 2, FD is the criterion of minimization of the volatility of each generator individually, OS are the maximum amplitude of volatility, US is undershooting and T_s is time settling, and N_G is the number of generators. It can be stated that ISTSE is a suitable

criterion for damping interregional volatility while FD minimizes the volatility of each generator separately.

3. Ant Colony Optimization Algorithm

The ant colony optimization algorithm, abbreviated as ACO, is known as the ant colony algorithm and ant colony optimization. This method is derived from the ant real movement in nature, which was first introduced in Dr Marco Drigo's thesis in 1990 entitled Ant System. The behavior of ants in their colonies is more to maintain colony survival.

One of the most important and interesting research on the behavior of living things such as ants (animals that are blind) is how they find food and the shortest route from their colonies to food sources. This sort of behaviour has a kind of mass intelligence that has been considered by scientists recently. In the ant colony algorithm, the seeker particles are a limited number of synthetic ants that exploit the Stigmage correlation, i.e., a form of indirect relation that is used by the environment to construct the answers to the problem.

After thoroughly observing the ant's behaviour and carrying out the necessary practical investigations, it was concluded that all the ants leave substances called pheromones when walking. The secretion rate of this substance is completely determined and evaporates after a time. The ants can detect pheromones through their sense of smell. They also choose a path that has a higher pheromone concentration between the two paths. Suppose there are two paths between an ant's nest and a food source, one path to be shorter than the other. One of the ants goes through the shorter path and the another through a longer path and these choices are completely random. Both ants leave their pheromones in the path. Certainly, an ant that has gone the shorter path, gets to the food source first, picks up some food and returns to the nest. When he reaches the nest, he places the food in the nest and goes back to the food source. But the ant that has gone the long way may still be on its way to the food source, so it will probably come back to the nest later than the ant that took the shorter path. So, the shorter path will have more pheromones, therefore, other ants looking for a way to find the food source will choose the shorter path because the pheromone concentration is higher on that path. Likewise, after a certain amount of time, most ants go through the shorter path. Following the features mentioned for the ants, the structure of the ACO algorithm will be discussed [39].

3.1. Ant Colony Algorithm

An ACO problem can be described as follows:

Suppose the ant colony contains N ants. The ants started moving from the house as shown in Figure 1. In each iteration or period, each ant will travel from the first layer to the last layer to reach its destination (food). Each ant in each layer can only select one option with probability P_{ij} according to the following equation.

$$P_{ij}^K = \begin{cases} \frac{(\tau_{ij})^\alpha}{\sum_{j \in N_i} (\tau_{ij})^\alpha} & \text{if } j \in N_i \\ 0 & \text{if } j \notin N_i \end{cases} \quad (3)$$

Where τ_{ij} is the intensity of the pheromone left on the path in ij . α indicates the importance of pheromone. N_i shows the number of neighbouring locations for the k ant. And j is the next place of ant k .

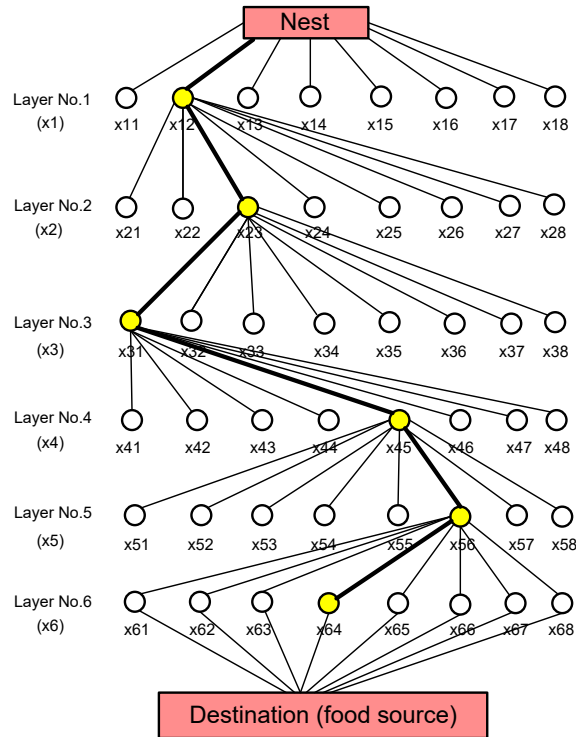


Figure 1: How to find the path between the nests to the source of food in a multivariate problem by ants

At the beginning of the optimization process, all pathways have an initial pheromone concentration. As shown in Figure 1, the ants began to move from their nest and randomly searched for a variable in each layer. In each iteration, each ant will traverse a response vector (the path traversed by the ant) consisting of search variables that are between the nest and the food. This search will continue until the maximum iteration. The value of each variable is selected as the optimal component of the answer vector based on the path that has the most pheromones. And in the end, almost all ants choose the best path that has the most pheromones. The k ant when in place i uses T_{ij} value to select the next location (j) which will calculate the probability of choosing each location from Equation 4. The selected points along the path by each ant are the candidate to answer the problem. For

example, a path traversed by the k ant is illustrated in Figure 1, where the answers x_{12} , x_{23} , x_{31} , x_{45} , x_{56} , x_{64} form a complete path between the nest and the food source. Each ant leaves some pheromone in its path. The following formula shows the increase in pheromone concentration after each ant crosses between i and j locations [39].

$$\tau_{ij}^{(k)} \leftarrow \tau_{ij}^{(k-1)} + \Delta\tau^{(k)} \quad (4)$$

When ant k moves in a path, the pheromone will be evaluated in all directions by the following formula:

$$\tau_{ij} \leftarrow (1-\rho)\tau_{ij} \quad \forall (i, j) \in A \quad (5)$$

Where ρ is the evaporation coefficient and a value in the range of $[0,1]$. A is the path from the nest to the feed source. Considering that the evaporation factor causes the weaker answers to be omitted, this will make the search process to be more dynamic, as there may be other shorter paths. An iteration of the search process involves ants moving, pheromone evaluation, and pheromone residual value. Upon return of all ants, the pheromone nest will be updated according to the following formula:

$$\tau_{ij} = (1-\rho)\tau_{ij} + \sum_{k=1}^N \Delta\tau_{ij}^{(k)} \quad (6)$$

Where $\Delta\tau_{ij}^{(k)}$ is the amount of pheromone left on the arc ij by the superior ant k . The pheromone left on the ij path is obtained by the best ant:

$$\Delta\tau_{ij}^{(k)} = \frac{Q}{L_k} \quad (7)$$

Where Q is a constant value and L_k is the length of the path traveled by the k ant (in the case of traveling from one city to another in the problem of itinerant sale). Equation 7 can be executed as follows:

$$\Delta\tau_{ij}^{(k)} = \begin{cases} \frac{\alpha f_{best}}{f_{worst}}; & \text{if } (i, j) \in \text{globalbest tour} \\ 0; & \text{otherwise} \end{cases} \quad (8)$$

Where f_{worst} is the worst value and f_{best} is the best value of the objective function among paths traversed by N ant, and α is a parameter to control the pheromone update scale. The greater this value, the more pheromones will accumulate on the best global path, and the better algorithm will search for local optimizations, find the true optimization and will not be caught in local optimizations. The step-by-step ant colony algorithm for solving a minimization problem is summarized as follows [39]:

First step:

Suppose that there are N ants in a colony and that for each n variable, the locations contain discrete values to be determined. The allowed discrete values of the variable x_i are expressed as $x_{i1}, x_{i2}, \dots, x_{ip}$ ($i = 1, 2, \dots, n$). Suppose $\tau_{ij}^{(1)}$ is the initial pheromone value in

all the paths of Figure 2, superscript τ_{ij} expresses a repetition number. For example $\tau_{ij}^{(1)} = 1$ can be included for all paths in the first iteration.

Second step:

A) Calculating the probability of choosing the next path or the discrete value for the variable x_{ij}

$$p_{ij} = \frac{\tau_{ij}^{(l)}}{\sum_{m=1}^p \tau_{ij}^{(l)}}; \quad i = 1, 2, \dots, n; \quad j = 1, 2, \dots, p \quad (9)$$

The above equation is similar to Equation 3 where $\alpha = 1$. Larger values are also used for α .

B) In the next step, the cumulative probability will be calculated by using Equation 9 and can randomly select the best local position using the k roulette-wheel method. This will be done as follows:

N numbers are randomly generated $r_1, r_2, r_3, \dots, r_N$ in the range (0,1) per ant. It is compared with the cumulative probabilities and the cumulative probabilities that are greater than the number generated are selected and the relevant position will be considered as the best local position.

Third step:

A) Step 2b repetition for all variables $i = 1, 2, \dots, n$.

B) Evaluating the objective function by the values corresponding to a complete path (vector $X^{(k)}$ or x_{ij} values for all variables by the ant k):

$$f_k = f(X^{(k)}); \quad k = 1, 2, \dots, N \quad (10)$$

The best and worst Route selected path among the N path by ants:

$$f_{best} = \min\{f_k\} \quad k = 1, 2, \dots, N \quad (11)$$

$$f_{worst} = \max\{f_k\} \quad k = 1, 2, \dots, N \quad (12)$$

Fourth step:

Convergence occurs if almost all ants choose the best path. If convergence is not achieved, it is assumed that all ants will return home and begin their food search again. In this case, an iteration will be added ($l = l + 1$). And pheromone (or discrete values for variables) on paths will be updated as follows:

$$\tau_{ij}^{(l)} = \tau_{ij}^{(old)} + \sum_{k=1}^N \Delta\tau_{ij}^{(k)} \quad (13)$$

Where $\tau_{ij}^{(old)}$ is the pheromone value in the previous iteration (here the (l-1) iteration), which will be derived from the following formula:

$$\tau_{ij}^{(old)} = (1 - \rho)\tau_{ij}^{(l-1)} \quad (14)$$

And $\Delta\tau_{ij}^{(k)}$ is the pheromone left by the top ant k on its path and the sum of the pheromone on all paths by the top ants (if multiple ants provide top similar paths) will be considered. Note that the top path for variable i is only one path. The evaluation rate or evaporation coefficient ρ is in the range from 0.5 to 0.8.

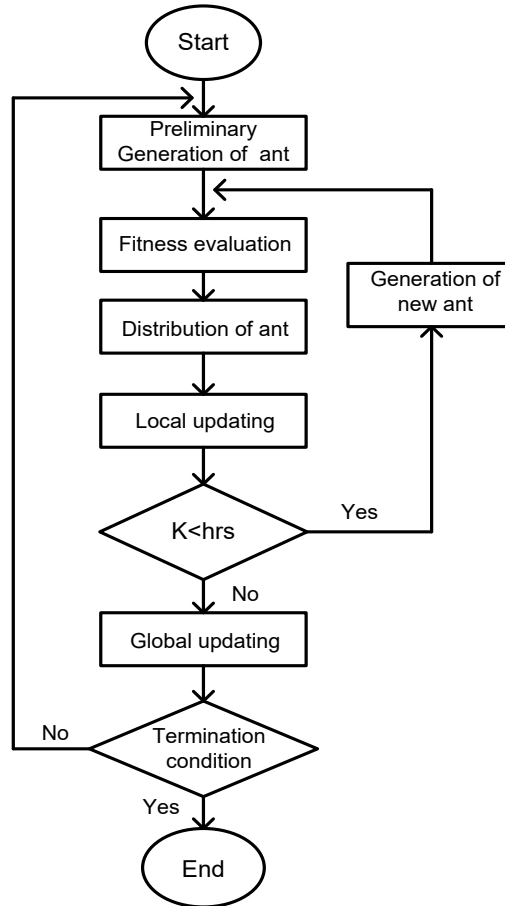


Figure 2: General Flowchart of Ant Colony Algorithm

The algorithm returns to the second step with the new value $\tau_{ij}^{(l)}$. Stages 2, 3 and 4 will be repeated until convergence. Convergence is achieved when all ants choose a path as the best path. In some cases, the repetition will stop after the maximum number of replications (l_{\max}). Figure 2 shows the general flowchart of the ant colony algorithm.

4. Simulation and Analysis of Results

In this section of the paper, we examine the results of simulation in the MATLAB software environment. Studies have been conducted to evaluate the effect of the presence of power system stabilizers and converter type series compensator in the transmission line (SSSC) under different loading conditions. For this purpose, a standard two-regional power system with two synchronous generators in each area is selected as the sample system. The single-linear block diagram is given in Figure 3. Generators in each area have nominal values of 900 MVA and 20 KV. A 900 MVA transformer with a conversion ratio of 20/230 KV was used for each unit. The two zones are connected by two lines [40-42].

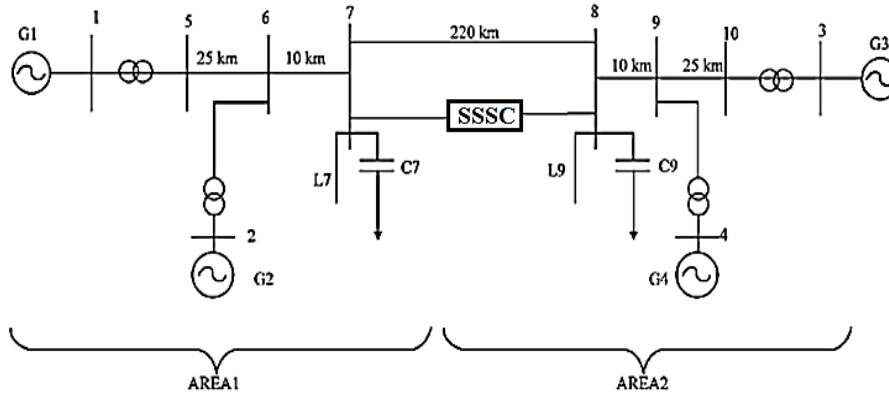


Figure 3: Single-linear block diagram of the system under study

In the studied system, the loads are modeled as constant impedances. In the system under study, the G_1 generator is considered as the reference generator. In the stimulation system of each of the generators, there is a stabilizer of the pre-phase and post-phase power system. It is also used in one of the communication lines between the two areas of the SSSC compensator. It should be noted that the SSSC compensator is installed in 110 kilometers from bus 7 and in the middle of the communication line between the two regions. The studies were repeated in two loading conditions where the active and reactive power output values of each generator are summarized in Table 1.

Table 1: System loading conditions (per-unit)

Generator	First scenario		Second scenario	
	P	Q	P	Q
G_1	0.78	0.15	1	0.26
G_2	0.77	0.26	0.08	0.42
G_3	0.78	0.14	0.75	0.15
G_4	0.77	0.22	0.77	0.27

To coordinate the parameters of the power system stabilizers as well as adjust the controller parameters in the SSSC compensator, the particle swarm algorithm, as well as the ant colony proposed algorithm, have been used. The parameters of these two algorithms are summarized in Table 2. The simulations will be repeated in the loading conditions referred to in Table 1 in the form of two scenarios. In each scenario, a comparison will be made between the controllers designed by the ACO and PSO algorithms, and finally, a comparison will be made between these methods. In Table 3, the optimal values of the SSSC stabilizer and controller parameters obtained by the ACO and PSO algorithms are presented.

Table (2): Parameters of ACO and PSO Algorithms

PSO	Population	Repetition	$C_1=C_2$	W	V_{min}	V_{max}
		100	50	2	0.7	0.4
ACO	Population	Repetition	α	β	P	
	100	50	0.8	0.2	0.7	

Table (3): Parameters optimized by ACO and PSO algorithms

ACO	Gen	K	T_1	T_2	T_3	T_4
	G1	18.32	0.42	0.36	0.76	0.39
	G2	28.4	0.21	0.86	0.51	0.63
	G3	20.36	0.32	0.17	0.47	0.63
	G4	23.71	0.89	0.76	0.39	0.94
	SSSC	K_p	K_i			
	1.8	0.7				
PSO	Gen	K	T_1	T_2	T_3	T_4
	G1	17.23	0.14	0.74	0.34	0.64
	G2	21.36	0.42	0.54	0.27	0.74
	G3	23.14	0.23	0.37	0.76	0.36
	G4	20.84	0.36	0.49	0.54	0.27
	SSSC	K_p	K_i			
	1.64	0.65				

To more accurately investigate the results of the simulations, the maximum values of the range of volatility, the damping time and the ISTSE and FD criteria were calculated. It should be noted that the settling time is calculated at 4% of the final value.

4.1. First scenario

In this scenario, the output power of the generators is adjusted according to Table 1. In these loading conditions, a three-phase error to the ground with 250 ms occurred at the communication line between the two shins 7 and 8 in the second. After optimal coordination of the stabilizers by PSO and ACO algorithms, their performance in the power system was evaluated. For this purpose, the angular velocity variations of the generators are presented below.

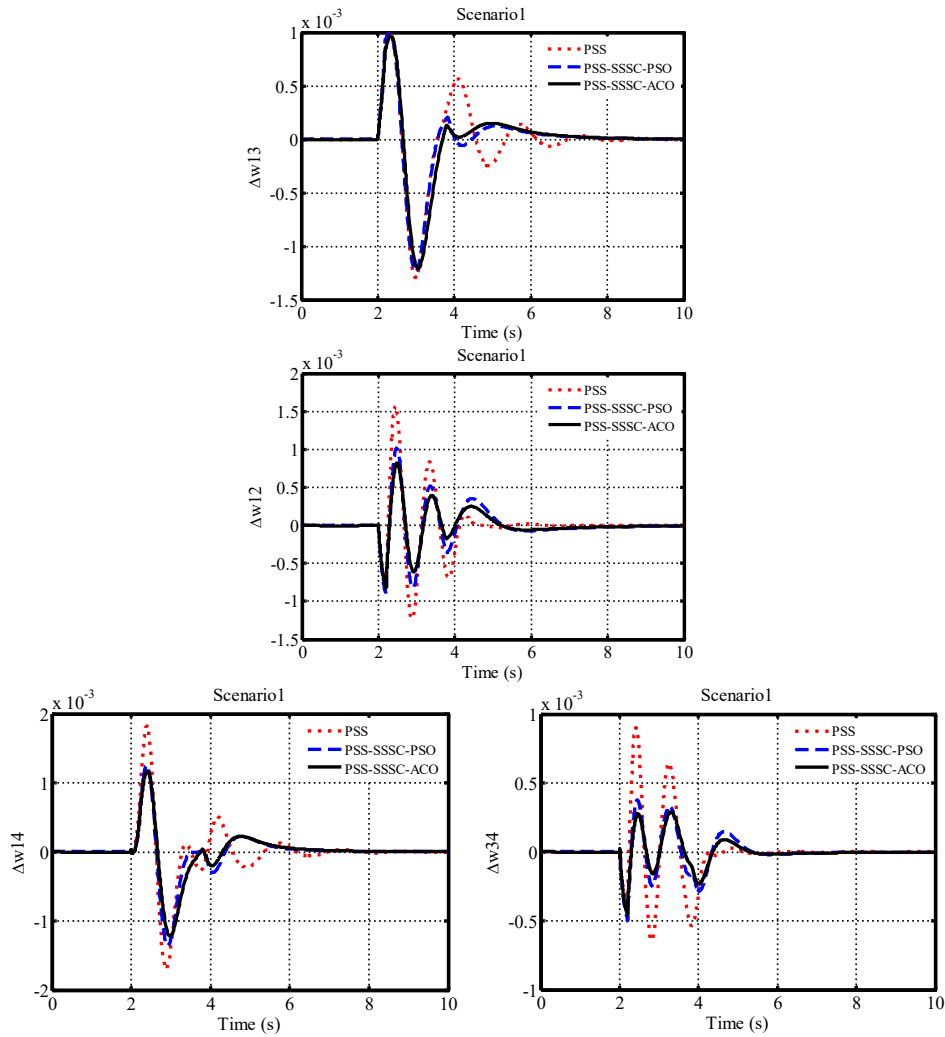


Figure 4: The angular velocity variations of the generators in the first scenario

In Figure 4, the angular velocity variations of the generators when using the PSS stabilizer alone are shown in red dots and when using the stabilizers with the SSSC compensator optimized by the PSO and ACO algorithms in blue and black lines, respectively. The objective function value (ISTSE) obtained for each of the control methods in Figure 5 is shown as a bar graph.

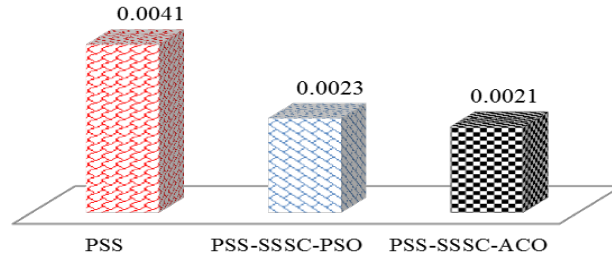


Figure 5: Objective function values in the first scenario

The objective function value (ISTSE) for the power system with stabilizer without SSSC is 0.0041, whereas this value is much lower using SSSC. The ISTSE value for the control system designed by the ACO algorithm is 0.0021 and if designed with the PSO algorithm, this value is 0.0023. These two values are approximated to each other, indicating a relatively similar performance of both algorithms. On the one hand, given the curves shown in Figure 4, we can properly consider the performance of each control method. For example, the maximum range of variations for a system using only a stabilizer is 0.186, which is the highest value. The maximum range of variations for the control system optimized by ACO and PSO algorithms is calculated to be 0.11 and 0.12, respectively. It should be noted that the maximum variation of all the curves in Figure 4 is chosen. This value is related to the angular velocity variations between generators one and four, i.e., $\Delta\omega_{14}$.

Another result of the simulation is the damping time of the volatility in the power system. In the power system, the more the stability, the volatility caused by disturbances damps faster and the system condition improves in terms of performance. For power systems with stabilizer and without SSSC, the settling time was calculated to be 5.64 seconds. Whereas the damping time for the power system with stabilizer and SSSC optimized by PSO and ACO algorithms were 4.46 seconds and 4.07 seconds, respectively. To calculate this criterion, like the maximum range criterion, the highest value was obtained among the four curves. The results show that the proposed control system has a lower damping time and range of lower volatility than the other two systems and it has been able to increase the stability of the system to a higher degree. The FD value for each control system is shown in Figure 6.

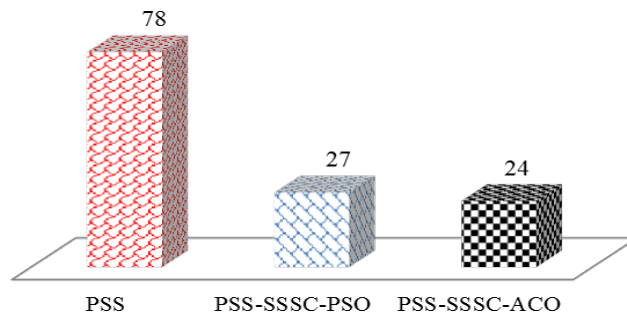
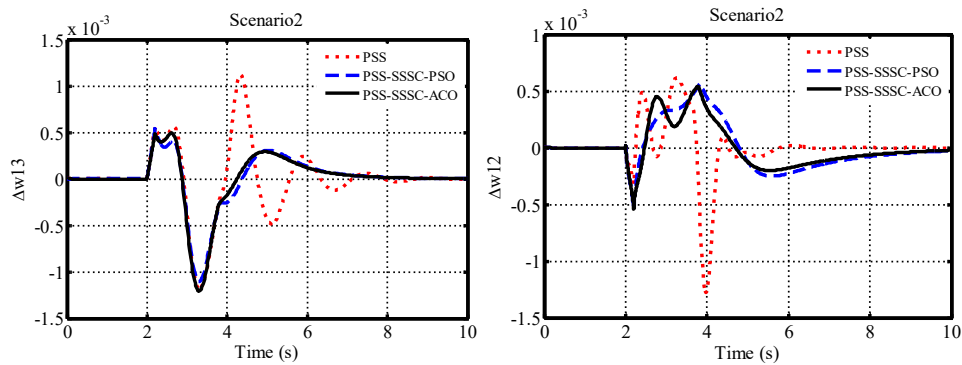


Figure 6: FD values in the first scenario

The FD value for the system with PSS stabilizer is 78, while for power systems in the presence of the SSSC line series compensator, this value is calculated as 27 and 24, respectively. The smaller FD value is the final confirmation of the performance of the proposed control system.

4.2. Second scenario

In the second scenario, the performance of the designed stabilizers is evaluated by changing the system loading conditions and increasing the output power of the generators. The active reactive power values of each generator in this scenario are presented in Table 1. In the loading conditions defined in the second scenario, as in the first scenario, a three-phase error to ground with 250 ms occurred in the communication line between the two regions. After optimization, the angular velocity curve of the generators is shown in Figure 7.



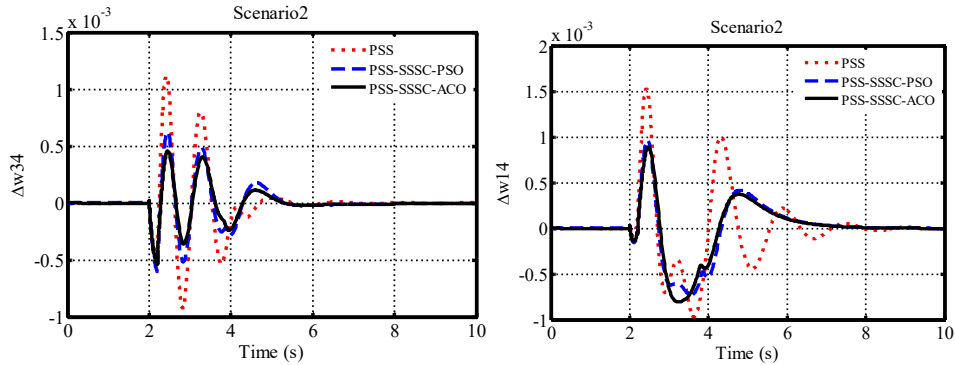


Figure 7: Angular velocity variations of generators in the second scenario

As in the first scenario, the values of the objective function are calculated as shown in Figure 8 as bar diagrams.

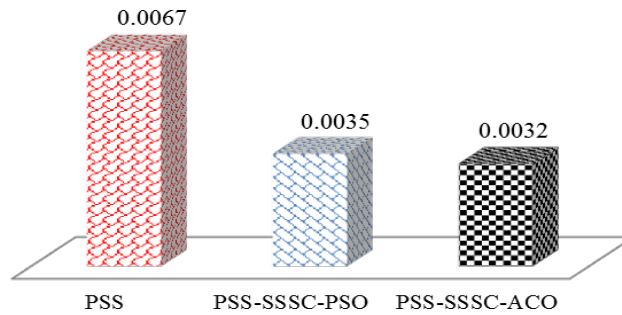


Figure 8: Objective function values in the second scenario

As it can be seen from the results, the control system designed using the ACO algorithm has a higher accuracy than the system designed by the PSO algorithm. This indicates the accuracy of the proposed ACO algorithm over other algorithms. Also, the value of the objective function in the presence of the SSSC series compensator is much lower than the system without the compensator. The lower the value of the objective function, the control system will be able to make volatility damping in less time and with less range. The angular velocity variation curve indicates that the control system proposed in this paper has less volatility than the other two control methods. The maximum amplitude of variation for the three control methods was 1.52, 0.91 and 0.73, respectively. Damping time of volatility for these three systems were 7.26, 5.68 and 5.12, respectively. The damping time of the power system in the presence of the PSS stabilizer and the SSSC compensator has a smaller value. In terms of dynamic stability, it can be said that the lesser the settling time, the more stable the system becomes. The FD criterion for the second scenario was then calculated. Figure 9 shows the bar diagram.

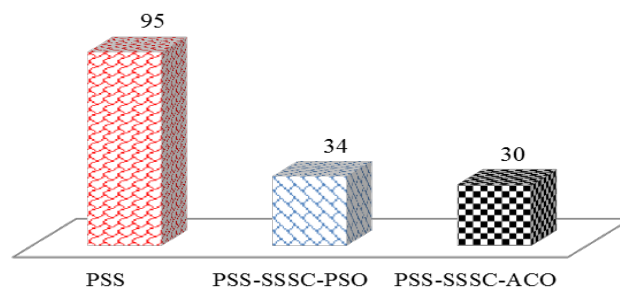


Figure 9: FD values in the second scenario

It should be noted that the lower the criterion value, the volatility dampens with lower range and in the shorter time. This is due to smallness of the FD criterion of the optimized control system in comparison to two other control systems when overshooting and undershooting or settling time in the system.

5. Conclusion

In this paper, the stability of a multi-machine power system is studied. For this purpose, a standard four-machine power system was selected as the study system. PSS stabilizers with SSSC series compensator were used in this system. Coordination of power system stabilizers and SSSC compensator parameters is optimized by PSO and ACO optimization algorithms and finally, under different loading conditions, studies were repeated. Simulations are performed by applying three-phase error to earth and the performance of the designed control systems is evaluated. To compare the performance of each of the proposed systems, the maximum overshoot, settling time, and FD criteria have been calculated. Knowing these values helps us to think about each system fairly; lower values indicate the better performance of the control system. Meanwhile, the FD criterion can be the best criterion for comparisons. Because at that time, the settling time, overshooting and undershooting are considered.

The results show that in the presence of series compensator, the stability margin of the system is increased and the criterion values are much lower than when no series compensator was used. If the PSS and SSSC are used simultaneously, the power system has a better condition and has been able to make volatility in different operating conditions with less amplitude and in a shorter damping time. The more the damping increases, the stability of the system increases, and the lines are able to transfer more power with the appropriate stability margin.

References

1. Fathizadeh, M., 'Power system stabilizer design for maximum stability margin,' Proc. of the Twenty-First Annual North-American. IEEE Power Symposium, pp. 168-174, Oct. 1989.
2. Hassan LH, Moghavvemi M, Almurib HAF, Muttaqi KM, Ganapathy VG., 'Optimization of power system stabilizers using participation factor and genetic algorithm', Int J Electr Power Energy Syst, vol. 55, pp. 2014; 668–79.

3. Mostafa H, El-Sharkawy M, Emary A, Yassin K. Design and allocation of power system stabilizers using the particle swarm optimization technique for an Inter connected power system. *Int J Electr Power Energy Syst* 2012;34(1):57–65 .
4. Keumarsi, V., et al. "An integrated approach for optimal placement and tuning of power system stabilizer in multi-machine systems." *International Journal of Electrical Power & Energy Systems* 2014; 63(0): 132-139.
5. Shayeghi, H., Safari, A., Shayanfar, H.A., ' PSS and TCSC damping controller coordinated design using PSO in multi-machine power system', *Energy Conversion and Management*, vol. 51, pp. 2010 ;2930-2937.
6. Mondal, D., Chakrabarti, A., Sengupta, A., ' Optimal placement and parameter setting of SVC and TCSC using PSO to mitigate small signal stability problem', *International Journal of Electrical Power & Energy Systems*, vol. 42, pp. 2012 ; 334-340.
7. Abd-Elazim SM, Ali ES. Coordinated design of PSSs and SVC via bacterial foraging optimization algorithm in a multi-machine power system. *Int J Electr Power Energy Syst* 2013; 41:44–53
8. Abd-Elazim S, Ali E. Power system stability enhancement via bacteria foraging optimization algorithm. *Arabian J Sci Eng* 2013; 38(3): 599–611
9. Tripathy M, Mishra S. Coordinated tuning of PSS and TCSC to improve Hopf Bifurcation margin in multi machine power system by a modified Bacteria Foraging Algorithm. *Electr Pow Energy Syst* 2015; 66:97–109.
10. Panda S, Yegireddy NK, Mohapatra SK. Hybrid BFOA–PSO approach for coordinated design of PSS and SSSC-based controller considering time delays. *Int J Electr Power Energy Syst* 2013; 49:221–33.
11. Abd-Elazim SM, Ali ES. A hybrid particle swarm optimization and bacterial foraging for optimal power system stabilizer design. *Electric Power Energy Syst* 2013; 46:334–41.
12. Esmaili MR, Hooshmand RA, Parastegari M, Ghaebi Panah P, Azizkhani S. New coordinated design of SVC and PSS for multi-machine power system using BF-PSO algorithm. *Procedia Technol* 2013; 11:65–74
13. W. Wang, H. Xu, M. Alazab, T. R. Gadekallu, Z. Han and C. Su, "Blockchain-Based Reliable and Efficient Certificateless Signature for IIoT Devices," in *IEEE Transactions on Industrial Informatics*, doi: 10.1109/TII.2021.3084753.
14. Wang, W., Huang, H., Zhang, L., & Su, C. (2020). Secure and efficient mutual authentication protocol for smart grid under blockchain. *Peer-to-Peer Networking and Applications*, 1-13.
15. Zhang, L., Zhang, Z., Wang, W., Jin, Z., Su, Y., & Chen, H. (2021). Research on a Covert Communication Model Realized by Using Smart Contracts in Blockchain Environment. *IEEE Systems Journal*.
16. Zhang, L., Zou, Y., Wang, W., Jin, Z., Su, Y., & Chen, H. (2021). Resource allocation and trust computing for blockchain-enabled edge computing system. *Computers & Security*, 105, 102249.
17. L. Tan, H. Xiao, K. Yu, M. Aloqaily, Y. Jararweh, "A Blockchain-empowered Crowdsourcing System for 5G-enabled Smart Cities", *Computer Standards & Interfaces*, <https://doi.org/10.1016/j.csi.2021.103517>
18. C. Feng, et al., "Efficient and Secure Data Sharing for 5G Flying Drones: A Blockchain-Enabled Approach", *IEEE Network*, vol. 35, no. 1, pp. 130-137, March/April 2021, doi: 10.1109/MNET.011.2000223.
19. Sambariya DK, Prasad R. Robust tuning of power system stabilizer for small signal stability enhancement using meta heuristic bat algorithm. *Int J Electr Power Energy Syst* 2014; 61:229–38
20. Ali, E. S. "Optimization of Power System Stabilizers using BAT search algorithm." *International Journal of Electrical Power & Energy Systems* 2014; 61(0): 683-690.

21. K. Yu, Z. Guo, Y. Shen, W. Wang, J. C. Lin, T. Sato, "Secure Artificial Intelligence of Things for Implicit Group Recommendations", *IEEE Internet of Things Journal*, 2021, doi: 10.1109/JIOT.2021.3079574.
22. Yin Zhang, et al., "Edge Intelligence in the Cognitive Internet of Things: Improving Sensitivity and Interactivity", *IEEE Network*, vol. 33, no. 3, pp. 58-64, 2019.
23. H. Li, K. Yu, B. Liu, C. Feng, Z. Qin and G. Srivastava, "An Efficient Ciphertext-Policy Weighted Attribute-Based Encryption for the Internet of Health Things," in *IEEE Journal of Biomedical and Health Informatics*, doi: 10.1109/JBHI.2021.3075995.
24. L. Zhen, Y. Zhang, K. Yu, N. Kumar, Y. Xie, "Early Collision Detection for Massive Random Access in Satellite-Based Internet of Things", *IEEE Transactions on Vehicular Technology*, doi: 10.1109/TVT.2021.3076015.
25. Z. Guo, et al., "Robust Spammer Detection Using Collaborative Neural Network in Internet of Things Applications", *IEEE Internet of Things Journal*, doi: 10.1109/JIOT.2020.3003802.
26. Eslami M, Shareef H, Khajehzadeh M. Optimal design of damping controllers using a new hybrid artificial bee colony algorithm. *Int J Electr Power Energy Syst* 2013; 52:42–54.
27. Shayeghi, H. and A. Ghasemi. A multi objective vector evaluated improved honey bee mating optimization for optimal and robust design of power system stabilizers. *International Journal of Electrical Power & Energy Systems* 2014; 62(0): 630-645.
28. Gholipour E, Nosratabadi M. A new coordination strategy of SSSC and PSS controllers in power system using SOA algorithm based on Pareto method. *Electrical Power and Energy Systems* 2015; 67: 462–471.
29. Jalayer R, Ooi B. Co-Ordinated PSS Tuning of Large Power Systems by Combining Transfer Function-Eigen function Analysis (TFEA), Optimization, and Eigenvalue Sensitivity. *IEEE Trans on power system* 2014; 29: 2672 – 2680.
30. Z. Guo, K. Yu, A. Jolfaei, A. K. Bashir, A. O. Almagrabi and N. Kumar, "A Fuzzy Detection System for Rumors through Explainable Adaptive Learning," *IEEE Transactions on Fuzzy Systems*, doi: 10.1109/TFUZZ.2021.3052109.
31. Khadanga R, Satapathy J. Time delay approach for PSS and SSSC based coordinated controller design using hybrid PSO–GSA algorithm. *Electrical Power and Energy Systems* 2015; 71: 262–273.
32. Mitra, S.; Bhattacharya, A.; Dey, P. Small Signal Stability Analysis in Co-Ordination with PSS, TCSC, and SVC. In *Proceedings of the International Conference on Computation of Power, Energy, Information and Communication (ICCPEIC)*, Chennai, India, 28–29 March 2018; pp. 434–441.
33. Shahgholian, G.; Movahedi, A. Power system stabiliser and flexible alternating current transmission systems controller coordinated design using adaptive velocity update relaxation particle swarm optimisation algorithm in multi-machine power system. *IET Gener. Transm. Dis.* 2016, 10, 1860–1868.
34. Dey, P.; Mitra, S.; Bhattacharya, A.; Das, P. Comparative study of the effects of SVC and TCSC on the small signal stability of a power system with renewables. *J. Renew. Sustain. Energy* 2019, 11, 033305.
35. Shahriar, M.S.; Shafiullah, M.; Rana, M.J. Stability enhancement of PSS-UPFC installed power system by support vector regression. *Electr. Eng.* 2018, 100, 1601–1612.
36. Choudekar, P.; Sinha, S.K.; Siddiqui, A. Optimal location of SVC for improvement in voltage stability of a power system under normal and contingency condition. *Int. J. Syst. Assur. Eng. Manag.* 2017, 8, 1312–1318.
37. Baadji, B.; Bentarzi, H.; Bakdi, A. Comprehensive learning bat algorithm for optimal coordinated tuning of power system stabilizers and static VAR compensator in power systems. *Eng. Optim.* 2020, 52, 1761–1779.

38. P. R. Nakhi and M. A. Kamarposhti, "Multi objective design of type II fuzzy based power system stabilizer for power system with wind farm turbine considering uncertainty", *Int. Trans. Electr. Energy Syst.*, vol. 30, no. 4, pp. e12285, Apr. 2020.
39. M. Dorigo & K. Socha, *An Introduction to Ant Colony Optimization*. T. F. Gonzalez (Ed.), *Approximation Algorithms and Metaheuristics*, CRC Press, 2007.
40. Kundur, P., 'Power system stability and control', McGraw-Hill, USA, 1994.
41. C. Iwendi, Z. Zhang and X. Du, "ACO based key management routing mechanism for WSN security and data collection," 2018 IEEE International Conference on Industrial Technology (ICIT), 2018, pp. 1935-1939, doi: 10.1109/ICIT.2018.8352482.
42. C. Iwendi, J. A. Ansere, P. Nkurunziza, J. H. Anajemba and Z. Yixuan, "An ACO-KMT Energy Efficient Routing Scheme for Sensed-IoT Network," *IECON 2018 - 44th Annual Conference of the IEEE Industrial Electronics Society*, 2018, pp. 3841-3846, doi: 10.1109/IECON.2018.8591489.